EPR study of Eu^{2+} in $Pb_{1-x}Eu_xSe$ layers grown on a Si substrate

X. Gratens*
Instituto de Física, Universidade de São Paulo, Caixa Postal 66.318, 05315-970 São Paulo, São Paulo, Brazil

S. Isber†
American University of Beirut, Department of Physics, Bliss Street, P.O. Box 11-0236 Beirut, Lebanon

S. Charar‡
Groupe d'Etude des Semiconducteurs, CNRS-UMR 5650, Université Montpellier II, Place Eugène Bataillon, 34095 Montpellier Cedex 5, France

(Received 2 May 2007; published 17 July 2007)

Electron paramagnetic resonance (EPR) of Eu^{2+} ions in $Pb_{1-x}Eu_xSe$ layers grown by molecular beam epitaxy on Si substrate has been investigated. The measurements were performed on layers with thickness around 1.5 μm and europium concentration $x=0.01$, 0.06, 0.08, and 0.10. The spin Hamiltonian (SH) parameters of the single ion anisotropy were obtained from the sample with $x=0.01$. Room temperature (300 K) EPR measurements showed that the site symmetry of the Eu^{2+} ions is cubic and the SH parameters were found to be $g=1.970\pm0.001$, $b_4=270.5\pm0.5$ MHz, and $b_6=-2.0\pm0.5$ MHz. However, at $T=4.2$ K, it was found that the cubic symmetry is axially distorted along the [111] direction, perpendicular to the layer surface. The change in the EPR spectra at 4.2 K was interpreted by incorporating an axial component in the SH with $b_2=-41\pm3$ MHz. The observed distortion was attributed to strain induced by thermal expansion caused by a mismatch between the layer and the substrate. For $x=0.01$, we also observed a partially resolved hyperfine structure due to the ^{151}Eu and ^{153}Eu isotopes and a structure of lines due to Eu-Eu pair spectra. For samples with higher Eu concentration $x=0.06$ and $x=0.08$, the spectrum consisted of the isolated Eu^{2+} ions EPR lines superimposed on a broad single isotropic line at $g\approx2$, which was attributed to signal from Eu clusters. For the sample with $x=0.10$, we only observed a single broad line centered on $g\approx2$. The number of single Eu^{2+} ions was determined from the EPR lines intensities at $T=300$ K. The results show that the distribution of the Eu^{2+} over the cation sites is not random.

DOI: 10.1103/PhysRevB.76.035203 PACS number(s): 75.50.Pp, 76.30.−v, 71.70.Gm

I. INTRODUCTION

Diluted magnetic semiconductors (DMSs) generally consist of a magnetic semiconducting material, such as II-VI or IV-VI, in which a small fraction of cations is replaced by magnetic rare-earth or transition metal ions. DMSs have unique properties that make them potential candidates for use in optoelectronic and spintronic applications.[1–4] The doping of the host material with magnetic ions is a prerequisite to change the characteristics of the pure crystal, such as the increase of the energy gap of the material and/or the change of carrier's concentration. One extensively studied class of DMS is based on II-IV materials in which some of the cations have been substituted by manganese.[5] Another group is based on lead salts (PbS, PbSe, PbTe) with rocksalt crystal structure, containing divalent europium ions.[6] Magnetic properties involving electron paramagnetic resonance (EPR) on bulk $Pb_{1-x}Eu_xSe$ samples have already been reported.[7–10] In all these works, the fine structure (FS) of the isolated Eu^{2+} ions (i.e., ions which have no nearest-neighbor-like ions) located on sites with cubic symmetry was reported. The EPR of isolated Eu^{2+} ions (singles) in $Pb_{1-x}Eu_xSe$ layers and superlattices grown by molecular beam epitaxy (MBE) on BaF_2 substrate was also reported by Gratens *et al.*[11] The results showed that the site symmetry of the Eu^{2+} ions remains cubic in the whole range of temperature from 300 down to 4.2 K.

In this paper, we present the study of the strain on $Pb_{1-x}Eu_xSe$ layers grown by MBE on Si substrate by means of EPR measurements. Furthermore, the distribution of the Eu ions over the Pb sites in $Pb_{1-x}Eu_xSe$ layers as well as the exchange interaction between Eu^{2+} ion will be evaluated.

II. EXPERIMENT

High quality epitaxial layers of $Pb_{1-x}Eu_xSe$ were grown by MBE. The layer growth was controlled by reflection high-energy electron diffraction using a 2300 Riber MBE system and effusion cells for PbSe and Eu. Four layers of $Pb_{1-x}Eu_xSe$ with $x=0.010$, 0.060, 0.080, and 0.10 and thickness of 1.6, 1.2, 1.6, and 2.0 μm, respectively, were used in the present study. The layers were grown on (111)-oriented Si substrate using a thin (80 Å) CaF_2 buffer layer to reduce the lattice parameters as well as the thermal-expansion-coefficient mismatch between the layer and the substrate.[12–14] The values of Eu concentration were determined by microprobe analysis, and the EPR measurements were carried out from 300 to 4.2 K using an *X*-band (9.54 GHz) Bruker spectrometer. The samples of approximately 2×4 mm^2 were oriented in the EPR cavity with the external magnetic field **H** parallel to the (011) plane of the $Pb_{1-x}Eu_xSe$ layer. The temperature was regulated with an Oxford gas flow system and was measured with a thermocouple.

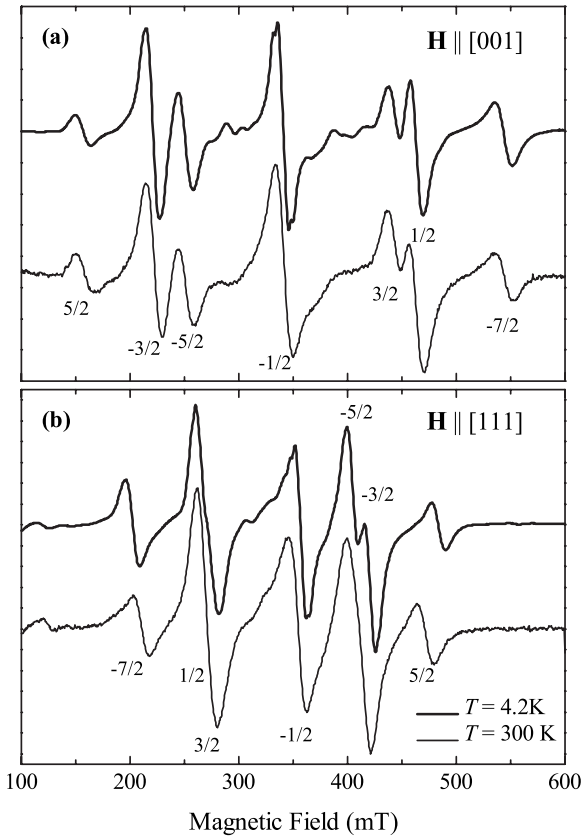

FIG. 1. X-band (9.56 GHz) EPR spectra for the $Pb_{1-x}Eu_xSe$ layer with $x=0.010$ at $T=300$ K and $T=4.2$ K: (a) the magnetic field direction is parallel to [001] and (b) **H** is perpendicular to the layer surface. In both directions, the fine structure (FS) lines of the isolated Eu^{2+} ions (singles) were identified by the quantum number m_S of the lowest energy level of the transition. For **H**||[111], the overall splitting of the FS was found to increase when the temperature was lowered down to 4.2 K, while for **H**||[001] no significant changes in the FS were perceived.

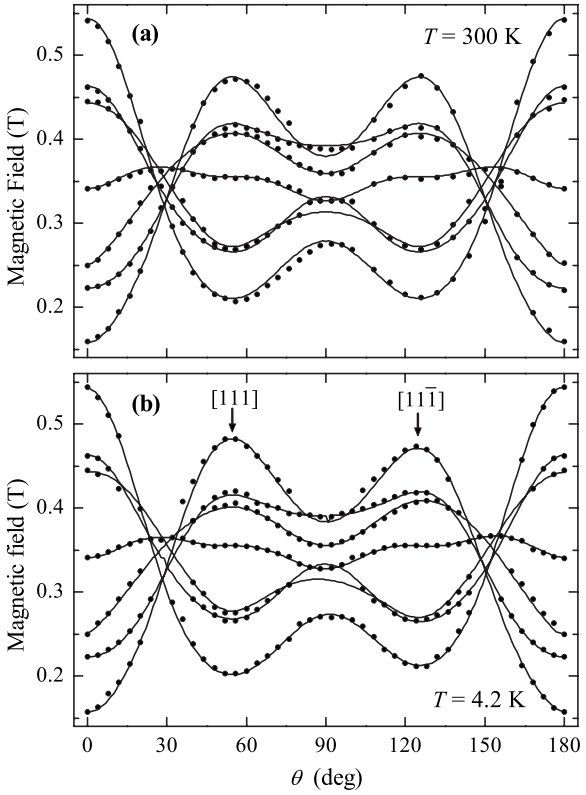

FIG. 2. Angular variation of the FS line positions with the magnetic field orientation at (a) $T=300$ K (b) and $T=4.2$ K for the layer with $x=0.010$. The magnetic field was rotated in the (011) plane of the $Pb_{1-x}Eu_xSe$ lattice. The orientation $\theta=0°$ correspond to the [001] direction. The circles represent the experimental data and the continuous lines are the best fits obtained by numerical matrix diagonalization of the spin Hamiltonian (SH). At $T=300$ K, the site symmetry of the isolated Eu^{2+} ions was found to be cubic, while at $T=4.2$ K, the cubic SH of Eq. (1) used at $T=300$ K was incremented by an axial symmetry term to account for the strain effect.

III. EPR SPECTRUM FOR LOW CONCENTRATION

In this section, we present the EPR results obtained for the layer with $x=0.010$. Due to the low concentration of the magnetic ions in this sample, the fine structure was well resolved and the effects of broadening as well as the correction due to demagnetization field were found to be insignificant. It is worthwhile mentioning that for this sample, EPR lines due to Eu-Eu pairs coupled by antiferromagnetic exchange interaction were also identified.

A. Fine structure of isolated ions

Figure 1 shows two relevant EPR spectra recorded at $T=300$ K for **H** parallel to the [001] direction and perpendicular to the layer (i.e., **H**||[111]). In both spectra, the seven FS lines corresponding to the allowed transitions $\Delta m_S=\pm 1$ (where m_S is the projection of the $S=7/2$ spin of Eu^{2+}) were clearly resolved. For both spectra, the transitions were identified based on the comparison of the experimental line intensities with theoretical values[15] at $T=300$ K and $T=4.2$ K. Furthermore, two EPR forbidden line ($\Delta m_S=\pm 2$) transitions were observed in the low-field part of the spectrum [Fig. 1(b)].

The angular dependence of the EPR line positions was recorded for various orientations of the external magnetic field in the (011) plane [Fig. 2(a)]. For each orientation of **H**, the positions of the FS lines were obtained from the fitting of the spectrum to seven EPR lines of Lorentzian shapes. Then, the collected FS line positions were simultaneously fitted to the spin Hamiltonian (SH) which describes the electronic states of the $^8S_{7/2}$ ion in cubic symmetry:[15]

$$\mathcal{H} = g\mu_B \mathbf{H}\cdot\mathbf{S} + \frac{b_4}{60}(O_4^0 + 5O_4^4) + \frac{b_6}{1260}(O_6^0 - 21O_6^4). \quad (1)$$

In Eq. (1), **H** is the external magnetic field and μ_B is the Bohr magneton. The spin operators O_m^n are those described by Abragam and Bleaney[15] and g, b_4, and b_6 are the usual SH parameters. The fitting of the data is shown in Fig. 2(a) and was obtained by numerical diagonalization of Eq. (1). The excellent agreement to the experiment confirms the cubic site symmetry of the isolated Eu ions. The SH parameters were found to be $g=1.970\pm0.001$, $b_4=270.5\pm0.5$ MHz, and

$b_6=-2.0\pm0.5$ MHz. These values are in very good agreement with those obtained for bulk crystals[7,9,10] and for layers deposited on BaF_2 substrate.[11]

The EPR spectra obtained at $T=4.2$ K for **H** parallel to the [001] and [111] directions are displayed in Fig. 1. For $\mathbf{H}\|[001]$, we clearly observe an increase in the intensity of the highest-field line compared to that of the lowest field line. This characteristic indicates that the transition within the two lowest energy levels $(-7/2\leftrightarrow-5/2)$ occurs at high field, while for $\mathbf{H}\|[111]$, due to the mixing of the energy levels, changes in the line position arrangement occur and the situation is inverted, i.e., the transition $(-7/2\leftrightarrow-5/2)$ becomes the lowest in field. This implies that at low temperatures, the levels with negative m_S are more populated than those with positive m_S, identifying the highest-field EPR line to be the $(-7/2\leftrightarrow-5/2)$ transition and the absolute sign of b_4 to be positive. Furthermore, for $\mathbf{H}\|[111]$, changes in the FS line positions were observed when the sample was cooled down to 4.2 K. These changes were characterized by an increase of the overall splitting of the spectrum and a wider separation between the two $(-1/2\leftrightarrow-3/2)$ and $(-3/2\leftrightarrow-5/2)$ EPR transitions, while for $\mathbf{H}\|[001]$, no significant changes in the FS line positions (within the experimental error) were observed. The positions of the FS lines were also determined at $T=4.2$ K for various orientations of the external magnetic field [Fig. 2(b)]. We clearly observed a deviation from the cubic symmetry, characterized by the nonequivalence of the directions [111] and $[11\bar{1}]$. The observed changes in the spectra are due to an axial distortion of the cubic symmetry along the [111] direction.[16] The data in Fig. 2(b) were fitted by matrix diagonalization of the cubic spin Hamiltonian of Eq. (1) incremented by the axial symmetry term of the form $\frac{b_2}{2}O_2^0$ with the z axis of the spin operator along the [111] direction, perpendicular to the surface of the layer. The fit was performed with b_2 as fitting parameter, while the values of g, b_4, and b_6 were used as determined from the measurements at 300 K. This choice was based on the fact that no relevant changes were observed for $\mathbf{H}\|[001]$. The best fitting to the experimental data was obtained for $b_2=-41\pm3$ MHz.

The observed axial distortion of the cubic symmetry at low temperature was attributed to the strain induced by thermal-expansion-coefficient mismatch between the substrate and the layer. At $T=300$ K, the site symmetry of the isolated ions was shown to be cubic, which is in agreement with a full relaxation of the strain after the growth of a thick layer.[14] On cooling the sample down to 4.2 K, and assuming the layer pinned to the substrate which deforms elastically, the lattice spacing parallel to the surface ($a_\|$) should be nearly constant $a_\|(T)=a(300\text{ K})=6.124$ Å due to the small thermal expansion coefficient of Si.[13] An exact calculation was made for $a_\|(4.2\text{ K})$ based on

$$a_\|(T)=a(300\text{ K})\left(\int_{300\text{ K}}^{T}\alpha dT-1\right). \quad (2)$$

In Eq. (2), α is the linear thermal expansion coefficient of Si instead of PbSe. We obtained $a_\|(4.2\text{ K})=6.122$ Å. The lattice parameter for "free" PbSe crystal is $a_0=6.094$ Å at 4.2 K, causing a tensile strain parallel to the interface $\varepsilon_\|=(a_\|-a_0)/a_0=0.46$ and a compressive strain $\varepsilon_\perp=-A\varepsilon_\|$ (with $A=1.16$).[14] The outcome of this strain is a rhombohedral deformation of the lattice with $\varepsilon_R=(a_\|-a_\perp)/a_0$, slightly higher than 1% at $T=4.2$ K. However, the changes in the FS line positions for $\mathbf{H}\|[111]$ were observed for $T<130$ K, implying a relaxation of strain between 300 and 130 K, while the layer deforms elastically only for $T<130$ K, in which case the calculation shows that the value of $b_2=-41\pm3$ MHz is correlated to a lattice deformation ε_R of 0.3%.

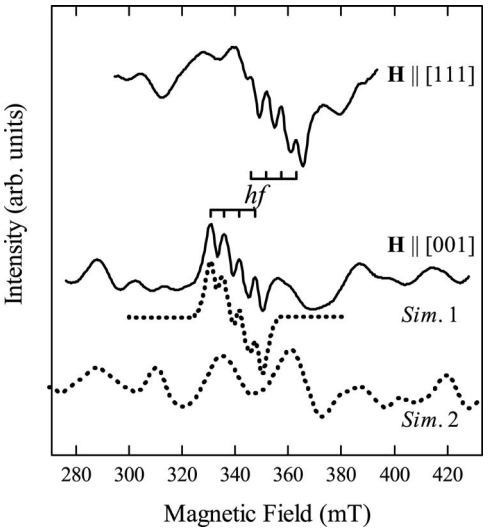

FIG. 3. $Pb_{1-x}Eu_xSe$ EPR spectra obtained at $T=4.2$ K for the layer with $x=0.010$, for $\mathbf{H}\|[001]$ and [111]. The solid lines represent the experimental spectra after subtractions of the central line. The traces exhibit a partially resolved hyperfine structure due to the isotopes ^{151}Eu and ^{153}Eu and another structure of much more broader linewidths attributed to Eu^{2+}-Eu^{2+} pairs. The dotted lines are the simulation results of the hyperfine structure (*Sim.*1) and the first nearest neighbor (NN) pair spectrum (*Sim.*2).

B. Other features of the EPR spectrum

Superimposed on the FS of the isolated Eu^{2+} ion spectrum, we have also observed other lines near the $(1/2\leftrightarrow-1/2)$ transition. The lines are clearly visible in Fig. 1 at $T=4.2$ K, but the overall structure is better resolved when a background line corresponding to the $(1/2\leftrightarrow-1/2)$ transition is subtracted from the spectrum as shown in Fig. 3.

We have identified the partially resolved hyperfine (hf) structure composed of four equally spaced lines due to the two equally abundant ^{151}Eu and ^{153}Eu isotopes. The positions of the hf lines determined from the second derivative of the absorption signal were also emphasized in Fig. 3 by vertical segments. The hf structure is the result of an overlap of 12 lines corresponding to both isotopes (six lines each). The analysis of the overall spacing of the structure and the position of the resolved lines allowed us to determine the hyperfine coupling constants to be $A(^{151}\text{Eu})=92.5$ MHz and $A(^{153}\text{Eu})=36$ MHz. These values were estimated from the

best simulation of the hf structure and were found to be in good agreement with the values reported in the literature for bulk samples containing Eu ions.[9,15]

Furthermore, other structures of lines in Fig. 3 were successfully identified within the energy levels of nearest neighbor (NN) Eu^{2+}-Eu^{2+} pairs coupled by antiferromagnetic (AF) exchange interaction. The dominant exchange interaction between Eu ions in $Pb_{1-x}Eu_xSe$ was found to be AF with a value of $J/k_B=-0.24$ K.[17] It was also established that the distribution of the Eu^{2+} ions over all the cation sites is near randomicity. Based on this result and for $x=0.01$, about 89% of the total number of Eu^{2+} ions are isolated and about 10% are NN exchange coupled ions. We have performed simulations of the NN pair spectrum for $\mathbf{H}\|[001]$ based on the appropriate pair spin Hamiltonian (PSH) given by

$$\mathcal{H}_{pair}=\mathcal{H}_{(1)}+\mathcal{H}_{(2)}-2J\mathbf{S}_1\cdot\mathbf{S}_2+d(3S_{1z}S_{2z}-\mathbf{S}_1\cdot\mathbf{S}_2), \quad (3)$$

where $\mathcal{H}_{(i)}$ $(i=1,2)$ corresponds to the low temperature SH for each of the two Eu^{2+} ions. The last two terms represent the isotropic exchange interaction $(J/k_B=-0.24$ K) and the dipolar interaction for the NN pairs, respectively.[17] When $\mathbf{H}\|[001]$, the dipolar interaction splits the 12 NN pairs into two nonequivalent NN groups, four pairs having their z axis (along the line joining the two ions) perpendicular to $\mathbf{H}$ and eight pairs making an angle of 45° with the [001] axis. However, for $\mathbf{H}\|[111]$, all the 12 NN pairs are equivalent. The dipolar constant d has been calculated using a point charge model with $d=(g\mu_B)^2/r^3$, where r is the distance between the two NN Eu ions without deformation of the cubic lattice.

In Eq. (3), the dominant term is the exchange interaction and the pair states can be described by the total spin $\mathbf{S}_T=\mathbf{S}_1+\mathbf{S}_2$.[18] The anisotropic terms in the Hamiltonian produce small splitting of the $(2S_T+1)$-fold degeneracies, giving rise to a structure of lines. We have determined the positions of the transitions by matrix diagonalization of the (64×64) PSH given in Eq. (3). For each transition, we have calculated the respective transition probability represented by the term $I_L=|\langle S_1,S_2,m_1,m_2|Sx_1+Sx_2|S_1',S_2',m_1',m_2'\rangle|^2$ using the eigenvectors of the PSH matrix for each of the magnetic field line transitions. The result showed that the main transitions occur between states of the same S_T and for $\Delta M_T=\pm1$ (where ΔM_T is the component of S_T along the external magnetic field), and it was concluded that the transition probabilities are proportional to $S_T(S_T+1)+M_T(M_T+1)$. Other transitions with much lower but significant transition probability have also been identified. It was found that they arise from energy levels with $\Delta S_T=0$ and $\Delta M_T=\pm2$. The simulation of the pair spectrum was performed at $T=4.2$ K, and the intensity of each of the lines was premeditated by the transition probability given by the term I_L and the Boltzmann population of the energy levels. The simulated pair spectrum shown in Fig. 3 was obtained by using a Lorentzian EPR line shape and a peak to peak width of $\Delta H_{pp}=9$ mT. The matching between the experimental and simulated spectra was not perfect but relatively good considering that no adjustable parameters were used in the simulation. The effect of the lattice distortion on the dipolar interaction has also been investigated; however, it turns out that the contribution of this term is negligible and brings no significant changes to the simulated pair spectra shown in Fig. 3. The slight disagreement between the experimental and simulated pair spectra could be due to a larger deviation from cubic symmetry around the two Eu^{2+} ions, which was not included in Eq. (3).

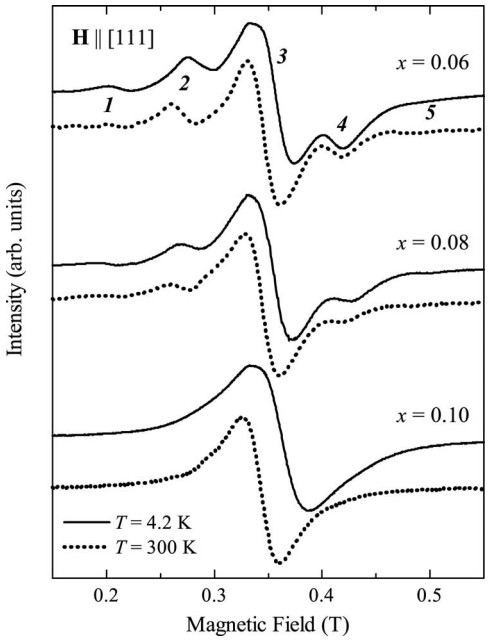

FIG. 4. EPR spectra of the samples with $x=0.06$, 0.08, and 0.10 obtained at $T=300$ K and $T=4.2$ K for $\mathbf{H}\|[111]$. The lines labeled 1, 2, 4, and 5 correspond to the FS of isolated Eu^{2+} ions. For $x=0.06$ and $x=0.08$, the central broad line labeled 3 is the result of the overlap of the $(-1/2\leftrightarrow+1/2)$ line of isolated Eu^{2+} ions and the AF cluster lines $(x=0.10)$.

IV. EPR ON LAYERS WITH HIGH Eu CONCENTRATIONS

A. Overall view

Figure 4 shows the EPR spectra collected for the layers with $x=0.060$, 0.080, and 0.10 at $T=300$ K and $T=4.2$ K with the external magnetic field along the [111] direction. For the three samples, the spectra show a broad line with $g\approx2$ labeled as number 3 on the graph. For $x=0.060$ and $x=0.080$, the FS lines from the isolated Eu^{2+} ions were also resolved. These lines were labeled on the graph as lines 1, 2, 4, and 5 in order of increasing field for $\mathbf{H}\|[111]$. Lines 2 and 4 in the spectra of $x=0.060$ and $x=0.080$ are the results of the overlap between the $(\pm5/2\leftrightarrow\pm3/2)$ and $(\pm3/2\leftrightarrow\pm1/2)$ lines. Lines 1 and 5 which correspond to the $(-7/2\leftrightarrow-5/2)$ and $(7/2\leftrightarrow5/2)$ transitions, respectively, were only observed for $\mathbf{H}\|[111]$. The relative intensity of line 3 as compared to the intensities of the other observed lines was found to increase with increasing x. For $x=0.10$, the spectrum consisted only of the isotropic central transition (line 3), as shown in Fig. 4.

The variation in the EPR spectra with increasing Eu concentration is attributed to the decrease in the number of singles and the increase of the AF clustering of Eu ions in the sample. Thus, for samples with large Eu concentration, line 3

is mainly due to signal coming from various types of AF clusters including pair contributions (Sec. III B).

B. Line positions and linewidths

An accurate determination of the SH parameters for the samples with $x=0.06$ and $x=0.08$ was difficult due to the large broadening and the overlap between various lines of the FS. However, simulation of the spectra by using the SH parameters determined at $T=300$ K for $x=0.010$ describes well the FS spectra of isolated Eu^{2+} ions for the samples with large concentrations, except for line 3 which is the superposition of the $(-1/2\leftrightarrow+1/2)$ and the AF cluster isotropic lines.

On cooling down to low temperature, we observed a shift in the line positions to higher field; this shift $\Delta H=H(4.2\ \mathrm{K})-H(300\ \mathrm{K})$ was found to increase with increasing x. For line 3, ΔH was found to be 11.0, 12.0, and 19.0 mT for $x=0.06$, 0.08, and 0.10, respectively. We have also noticed that ΔH is maximal for **H** perpendicular to the layer surface and increases with increasing the applied external magnetic field. The shift in the line positions was attributed to the demagnetization field caused by the sample shape. For **H** perpendicular to the layer surface, the internal field (H_{int}) within a flat sample is given by $H_{int}=H_{ext}-4\pi M$, where M is the sample magnetization.[19] At $T=300$ K and for $\mathbf{H}\|[111]$, the magnetization is expected to be small and the line shift would be given by $\Delta H=4\pi M$ at $T=4.2$ K. We calculated the expected shift for line 3 at $T=4.2$ K, assuming a pure paramagnetic film; the calculations were made by using a Brillouin function and yield $\Delta H=11.7$, 15.7, and 20.0 mT for $x=0.06$, 0.08, and 0.10, respectively. These values are slightly higher than the experimental values obtained from the EPR spectra, which is consistent with the presence of a weak AF clustering.

After correction of the demagnetization field, we were able to substantiate the presence of thermal strain for the layers with $x=0.06$ and $x=0.08$ from the overall splitting between lines 1 and 5 for $\mathbf{H}\|[111]$ and using the cubic SH parameters determined for $x=0.010$. Thus, the estimated b_2 values were −0.04 and −0.06 GHz for $x=0.06$ and $x=0.08$, respectively.

The EPR linewidths of the FS are originated by an intrinsic linewidth as well as dipolar and hyperfine broadening. According to this scheme, the linewidths are expected to be the same for all the FS lines. However, experimentally, the extreme FS lines (i.e., lines 1 and 5) for $x=0.010$ are characterized by larger linewidths as compared to the central line. It was found that $\Delta H_{pp}(+7/2\leftrightarrow+5/2)=14.5$ mT, $\Delta H_{pp}(-7/2\leftrightarrow-5/2)=16.0$ mT, and $\Delta H_{pp}(-1/2\leftrightarrow-1/2)=11.6$ mT for $\mathbf{H}\|[001]$ at $T=4.2$ K. This broadening of the extreme FS lines was attributed to a distribution of the SH parameters caused by the strain. To illustrate this difference, we have simulated the observed broadening of the satellite lines by assuming a Gaussian distribution of the parameter b_4 and using ΔH_{pp} of the $(-1/2\leftrightarrow-1/2)$ transition as the intrinsic linewidth (this approximation is valid, since, in first order, the axial component has no effect on the line positions for $\mathbf{H}\|[001]$). Good agreement between the simulated and experimental linewidth values was obtained for a half width $\Delta b_4=0.026b_4$. This value also gave a good description of the FS for $\mathbf{H}\|[111]$. For $x=0.06$ and $x=0.08$, the estimations of Δb_4 were not performed because of the lack of a good approximate for the intrinsic linewidth. Indeed, for these concentrations line 3 is mainly due to the AF clusters with a small contribution from the $(-1/2\leftrightarrow-1/2)$ line of the isolated ions. The line was found to have a Lorentzian line shape and broadens with decreasing temperature and increasing Eu concentration, which is a characteristic of exchange-narrowing cluster line also observed in other DMSs.[20–22]

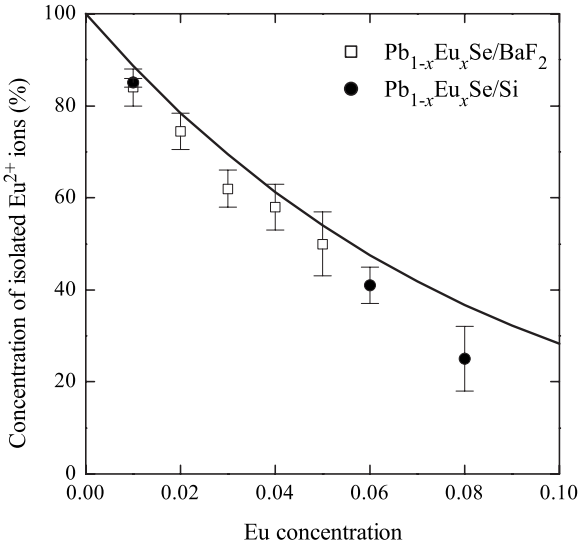

FIG. 5. Relative number of isolated Eu^{2+} ions in the $Pb_{1-x}Eu_xSe$ layers grown by MBE on Si (dark circle) and BaF_2 (open square) substrates. The continuous line represents the predicted number of singles assuming a random distribution of the Eu ions over the cation sites.

C. Concentration of the isolated ions

The number of single ions was estimated from the EPR line intensities at $T=300$ K for $\mathbf{H}\|[111]$ given by I_2, I_3, and I_4 for lines 2, 3, and 4, respectively. The intensity I_2 (or I_4) is related to the number of isolated Eu^{2+} ions $n(\mathrm{S})$, by $n(\mathrm{S})=I_2/27$, while the rest of Eu^{2+} ions considered to gather in various forms of AF clusters (i.e., pairs, open triplets, close triplets, and clusters with more than three coupled ions). The intensity of the AF clusters is given by $n(\mathrm{AF})=I_{AF}/84$, where I_{AF} was determined by subtracting from the intensity of line 3 the contribution of the FS $(1/2\leftrightarrow-1/2)$ line given by $I(1/2\leftrightarrow-1/2)=16I_2/27$. The relations given above are based on the theoretical intensity for the FS lines of isolated ions and assuming that the intensity for Eu^{2+} ions in a cluster is the same as that in the isolated ions at $T=300$ K. It is worthwhile mentioning that the experimental intensities were calculated by numerical integration of the absorption area. In Fig. 5, the relative numbers of singles given by $P(\mathrm{S})=n(\mathrm{S})/[n(\mathrm{S})+n(\mathrm{AF})]$ are plotted as function of the total Eu concentration for the four studied samples. The results obtained for epitaxial layers of $Pb_{1-x}Eu_xSe$ grown on BaF_2 sub-

strate are also displayed on the same figure. These data were compared to the number of relative Eu isolated ions deduced by assuming a random distribution of the ions over the site of Pb (continuous line in Fig. 5). The results clearly show a deviation from a random distribution toward a slight increase of AF europium clusters in the sample.

V. CONCLUSION

The EPR study of $Pb_{1-x}Eu_xSe$ $(0.01 \leqslant x \leqslant 0.1)$ layers grown by MBE on Si substrate confirms the substitution of Eu^{2+} on Pb^{2+} sites. At low temperature, the anisotropy caused by thermal strain was identified, measured, and compared to the cubic anisotropy. We have also investigated the rhombohedral deformation of the lattice arising at low temperature; the lattice deformation parameter was estimated to be $\varepsilon_R = 0.3\%$ at $T = 4.2$ K. EPR lines due to nearest neighbor pairs were clearly identified for the sample with $x = 0.01$. For higher Eu concentrations, the antiferromagnetic exchange interaction was also confirmed by the reduction in the isolated ion population. The intensity line calculation shows that the distribution of europium ions is close to being, but not perfectly, random. This was also confirmed for bulk samples of $Pb_{1-x}Eu_xX$ $(X = Te, Se, S)$[17,23,24] and $Sn_{1-x}Eu_xTe$.[25]

ACKNOWLEDGMENTS

This work was supported by the Brazilian agencies CNPq and FAPESP and the Arab Fund for Social and Economic Development (AFSED).

*xavier@if.usp.br
†Present address: Department of Physics and Astronomy, Tufts University, Medford, Massachusetts 02155, USA.
‡salam.charar@univ-montp2.fr

[1] G. Springholz, T. Schwarzl, W. Heiss, T. Fomherz, G. Bauer, M. Aigle, H. Pasher, and I. Vavra, Physica E (Amsterdam) **13**, 876 (2002).
[2] G. Grabecki, J. Wrobel, T. Dietl, E. Papis, E. Kaminska, A. Piotrowska, G. Springholz, and G. Bauer, Physica E (Amsterdam) **13**, 649 (2002).
[3] P. Banerjee, J. Pal, and B. Ghosh, J. Mater. Sci. **40**, 1333 (2005).
[4] G. Bauer and H. Pascher, in *Diluted Magnetic Semiconductors*, edited by M. Jain (World Scientific, Singapore, 1991).
[5] See, e.g., in *Semimagnetic Semiconductors and Diluted Magnetic Semiconductors*, edited by M. Averous and M. Balkanski (Plenum, New York, 1991); in *Diluted Magnetic Semiconductors*, edited by J. K. Furdyna and J. Kossut, Semiconductors and Semimetals Vol. 25 (Academic, New York, 1988); T. Dietl, in *Handbook on Semiconductors*, edited by T. S. Moss (North-Holland, Amsterdam, 1994), Vol. 3b, p. 1251.
[6] G. Bauer and H. Pascher, in *Semimagnetic Semiconductors and Diluted Magnetic Semiconductors*, edited by M. Averous and M. Balkanski (Plenum, New York, 1991), p. 209ff.
[7] G. B. Bacskay, P. J. Fensham, I. M. Ritchie, and R. N. Ruff, J. Phys. Chem. Solids **30**, 713 (1969).
[8] J. H. Pifer, Phys. Rev. **157**, 272 (1967).
[9] S. Isber, S. Charar, C. Fau, V. Mathet, M. Averous, and Z. Golacki, Phys. Rev. B **52**, 1678 (1995).
[10] S. Isber, S. K. Misra, S. Charar, X. Gratens, M. Averous, and Z. Golacki, Phys. Rev. B **56**, 13724 (1997).
[11] X. Gratens, A. B. Arauzo, G. Breton, S. Charar, M. Averous, and S. Isber, Phys. Rev. B **58**, 877 (1998).
[12] S. I. Novikova and N. Kh. Abrikosov, Sov. Phys. Solid State **5**, 1397 (1964).
[13] G. A. Stack and S. F. Bartram, J. Appl. Phys. **46**, 89 (1975).
[14] H. Zogg, S. Blunier, A. Fach, C. Maissen, P. Müller, S. Teodoropol, V. Meyer, G. Kostorz, A. Dommann, and T. Richmond, Phys. Rev. B **50**, 10801 (1994).
[15] A. Abragam and B. Bleaney, *Electron Paramagnetic Resonance of Transitions Metal Ions* (Oxford University Press, New York, 1970).
[16] E. R. Feher, Phys. Rev. **136**, A145 (1964).
[17] V. Bindilatti, N. F. Oliveira, Jr., Y. Shapira, G. H. McCabe, M. T. Liu, S. Isber, S. Charar, M. Averous, E. J. McNiff, Jr., and Z. Golacki, Phys. Rev. B **53**, 5472 (1996).
[18] M. T. Hutchings, R. J. Birgeneau, and W. P. Wolf, Phys. Rev. **168**, 1026 (1968).
[19] C. Kittel, Phys. Rev. **73**, 155 (1948).
[20] E. Chikoidzea, H. J. von Bardelebenb, Y. Dumont, P. Galtier, and J. L. Cantin, J. Appl. Phys. **97**, 10D316 (2005).
[21] P. R. Dorain, Phys. Rev. **112**, 1058 (1958).
[22] J. K. Furdyna and N. Samarth, J. Appl. Phys. **61**, 3526 (1987).
[23] E. ter Haar, V. Bindilatti, N. F. Oliveira, Jr., G. H. McCabe, Y. Shapira, Z. Golacki, S. Charar, M. Averous, and E. J. McNiff, Phys. Rev. B **56**, 8912 (1997).
[24] V. Bindilatti, E. ter Haar, N. F. Oliveira, Jr., M. T. Liu, Y. Shapira, X. Gratens, S. Charar, S. Isber, P. Masri, M. Averous, Z. Golacki, and E. J. McNiff, Phys. Rev. B **57**, 7854 (1998).
[25] X. Gratens, E. ter Haar, V. Bindilatti, N. F. Oliveira, Jr., Y. Shapira, M. T. Liu, Z. Golacki, S. Charar, and A. Errebbahi, J. Phys.: Condens. Matter **12**, 3711 (2000).